

Review

When the Total Hip Replacement Fails: A Review on the Stress-Shielding Effect

Davide Savio  and Andrea Bagno  *

Department of Industrial Engineering, University of Padova, 35131 Padova, Italy;
davide.savio.3@studenti.unipd.it

* Correspondence: andrea.bagno@unipd.it

Abstract: Total hip arthroplasty is one of the most common and successful orthopedic surgeries. Sometimes, periprosthetic osteolysis occurs associated with the stress-shielding effect: it results in the reduction of bone density, where the femur is not correctly loaded, and in the formation of denser bone, where stresses are confined. This paper illustrates the stress shielding effect as a cause of the failing replacement of the hip joint. An extensive literature survey has been accomplished to describe the phenomenon and identify solutions. The latter refer to the design criteria and the choice of innovative materials/treatments for prosthetic device production. Experimental studies and numerical simulations have been reviewed. The paper includes an introduction to explain the scope; a section illustrating the causes of the stress shielding effect; a section focusing on recent attempts to redefine prosthetic device design criteria, current strategies to improve the osteointegration process, and a number of innovative biomaterials; functionally graded materials are presented in a dedicated section: they allow customizing prosthesis features with respect to the host bone. Conclusions recommend an integrated approach for the production of new prosthetic devices: the “engineering community” has to support the “medical community” to assure an effective translation of research results into clinical practice.



Citation: Savio, D.; Bagno, A. When the Total Hip Replacement Fails: A Review on the Stress-Shielding Effect. *Processes* **2022**, *10*, 612. <https://doi.org/10.3390/pr10030612>

Academic Editor: Antonino Recca

Received: 1 March 2022

Accepted: 19 March 2022

Published: 21 March 2022

Publisher’s Note: MDPI stays neutral with regard to jurisdictional claims in published maps and institutional affiliations.



Copyright: © 2022 by the authors. Licensee MDPI, Basel, Switzerland. This article is an open access article distributed under the terms and conditions of the Creative Commons Attribution (CC BY) license (<https://creativecommons.org/licenses/by/4.0/>).

Keywords: stress-shielding; total hip prosthesis; bone remodeling

1. Introduction

The main function of the hip joint is to provide dynamic support to the body weight, transmitting loads from the axial skeleton to the lower limbs. The hip plays a primary role in locomotion but it is exposed to many risks and damages that can lead to pathological conditions.

The hip joint can be surgically replaced with a prosthetic device: the surgery may require the total joint replacement (total hip arthroplasty, THA) [1], when both patient’s femoral head and acetabulum are removed, or the hemi-replacement when only a part of the joint is replaced. The hip resurfacing arthroplasty (HRA) is an alternative to the conventional THA: the femoral head is not removed, it is trimmed and capped with a smooth metallic surface [2].

First attempts to perform hip surgery (i.e., joint excision) date back to the eighteenth century in the United Kingdom [3] (this reference represents a very interesting review on the history of the early hip arthroplasty procedures). The earliest replacements of the hip joint were performed in Germany: in 1891, Professor Glück exploited ivory as a biomaterial for substituting the femoral head in patients whose joint had been damaged by tuberculosis [1]. Since then, the development of novel design and the exploration of new materials has progressed continuously; the first total hip arthroplasty in the modern era was carried out in the early 1960s by Sir John Charnley, an orthopedic surgeon whose prosthesis model is still the most frequently used [4]. Thus, Sir Charnley is considered the father of the modern THA.

Presently, hip replacement is one of the most common orthopedic operations and almost one million joint replacements are performed every year in the world. These numbers are inevitably going to grow with the increasing aging of the world population. Since 2000, the number of hip and knee replacements has increased rapidly in most OECD (Organization for Economic Co-operation and Development) countries. On average, hip replacement rates increased by 30% between 2007 and 2017 as a consequence of the rising incidence and prevalence of osteoarthritis, caused by aging and obesity [5]. In the United States, the total annual counts of THA is expected to increase by 75% in 2025 to 652,000 replacements; by 129% in 2030 to 850,000 replacements, and by 284% in 2040 to 1,429,000 replacements. Trends are similar for both total hip and total knee arthroplasty: replacements are slightly more frequent in women and in individuals aged between 45 to 64 and from 65 to 84 years [6].

THA is indicated in patients suffering from severe osteoarthritis, juvenile rheumatoid arthritis, and in people with compound fractures of the femoral head or bone cancer. The main objective of THA is the complete restoration of the original biomechanical balance of the coxofemoral joint. Hip replacement has to function under high mechanical loads for many years and the mechanical strength of the materials used, combined with their biocompatibility, is crucial [7].

Typical components of a total hip prosthesis are the cup (also called acetabular component, made of metallic or polymeric materials), the ceramic or polymeric liner, the femoral head (made of metals or ceramic materials), and the metallic femoral stem (Figure 1).

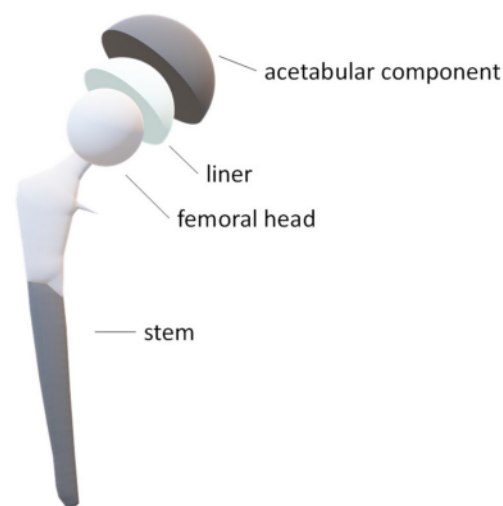


Figure 1. Sketch of the typical components of a total hip prosthesis.

The acetabular element can be a one-piece component (non-modular) or a two-piece component (modular). One-piece acetabular cups are typically made of ultra-high molecular weight polyethylene (UHMWPE) and are often fixed in the correct position with bone cement (polymethylmethacrylate, PMMA); alternatively, they are metallic and anchored to the bone thanks to porous metal or hydroxyapatite coating. Modular components consist of a metal shell and an insert made of UHMWPE, metal, or ceramic. The prosthesis can be fixed to the pelvic bones with orthopedic screws or nails. The femoral component, which consists of the femoral stem and femoral head, can also be modular or one-piece when the femoral head is coupled with the stem. Modular heads prostheses are made of CrCoMo alloys or ceramic materials, such as alumina (Al_2O_3) and zirconia (ZrO_2), which have a lower coefficient of friction but exhibit higher fragility. For the femoral stem, materials with high mechanical resistance are preferred, such as titanium alloys (Ti6Al4V), chromium-cobalt-molybdenum alloys (CrCoMo), or stainless steel. As in the case of the acetabular cup, fixation can be achieved with or without bone cement. The greatest advantage of bone cement is that it ensures stability immediately after surgery. Since the stability can

be accomplished regardless of bone quality, this technique is used in elderly patients, patients with bone tumors, or in revision surgeries, when a large amount of bone has to be removed. Major disadvantages of cemented THA are related to the poor mechanical properties of PMMA and to the heat developed by the polymerization reaction (highly exothermic). In the cementless procedure, the orthopedic surgeon excavates the medullary cavity of the femur to prepare a site that has the shape of the prosthesis but with a slightly smaller diameter; by forcing the stem into the cavity, the primary mechanical anchorage is established by a press fit. Secondary anchorage is obtained by means of osseointegration, which is promoted by the porous surface of the prosthesis. Non-cemented devices are more frequently used in young patients with very high physical demands, whom a prosthetic revision procedure is expected for [7].

Various are the possible causes of hip prostheses failure, including bone fracture, dislocation, deep vein thrombosis, pulmonary embolism, abductor muscle failure, wound complications, infection (septic mobilization), rupture of prosthetic components, wear and aseptic mobilization: the latter can be due to the stress-shielding phenomenon [8–11].

Generally speaking, periprosthetic bone loss caused by the stress shielding effect depends on both implant characteristics (design, materials, etc.) and bone quality. Mechanical-based models are useful for predicting bone adaptation and rely on mechanical stimuli such as stress, strain, and strain energy [12]. The latter is the most widely used: it will be described in the next section.

The work by Ravikant Sharma et al. [13] investigated the stresses at the interface between prosthetic stem and bone by means of FEA (Finite Element Analysis); the same group published a very recent paper [14] applying FEA to study stress distribution under dynamic conditions. A mechanobiological approach capable of predicting the long-term behavior of the femur after THA was proposed by Tavakkoli et al. [12]. Elsewhere, changes in postoperative bone density are quantified by Dual X-ray Absorptiometry (DXA), which provides a measure of bone mineral density (BMD) [15–17].

An established method to identify implants with a high risk of failure due to aseptic loosening is to measure the early migration of the femoral component by, for example, the “Ein Bild Roentgen Analyse” femoral component analysis (EBRA-FCA) [18]. Other researchers have recently focused on preoperative factors correlated with decreased periprosthetic BMD following THA, for example, the study by Morita et al. [19].

Methodological Approach and Scope

A literature survey through MEDLINE database was performed between October 2021 and March 2022. No date restrictions were specified. The search was performed with the terms “stress shielding”, “stress shielding total hip”, and “stress shielding THA”. MEDLINE returned 3593 items searching for “stress shielding”; this number decreased to 542 when the keywords were “stress shielding total hip” and to 182 with “stress shielding THA”. Google Scholar was also checked to extend the number of possible citations.

The results were refined to those with “prosthetic device”, “bone tissue mechanics”, “bone remodeling”, yielding more than 100 papers published between 1961 and 2022. Each paper was then selected for relevance and the article’s references were examined.

As it has been previously reported, THA surgery is one of the most common orthopedic surgery worldwide; nevertheless, incontrovertible strategies to limit the clinical impact of its complications are lacking. In particular, the present review is justified by the need to update the knowledge on both scientific and technological advances that have been exploited to investigate the causes of the stress shielding effect and to avoid/reduce its clinical impact. In particular, the review is aimed at illustrating investigations covering both experimental research and numerical simulations: the gap between the results of the scientific studies and their translation into the clinical practice is still a limiting factor for the successful reduction of the stress shielding effect.

This review does not cover the topics related to recent technological implementations in orthopedic surgery, e.g., virtual reality, computer navigation systems, and robotic-

assisted surgery. They are mentioned at the end of the conclusions to give the reader some hints on possible future developments.

2. Why Does the Stress-Shielding Appear?

Generally, the stress applied to the bone promotes its physiological remodeling in healthy individuals. This evidence had been expressed by Julius Wolff in the 19th century: his law describes the capacity of healthy bone to adapt to variable loading conditions [20].

The term “mechanosensation” has been recently introduced to indicate the ability of bone tissue to dynamically modify its morphology: new bone is added to withstand increased loads, whereas bone is resorbed when unloaded or disused [21]. The exact mechanism of bone adaptation to load has not been completely understood, but it is acknowledged that a number of stimuli can be detected by the osteocytes, which can sense the mechanical load and transduce it into a specific biological activity [22]. Osteocytes are terminally differentiated osteoblasts that reside within the bone matrix; they are sheltered into lacunae but still able to communicate with each other. Osteocytes play a fundamental role in mechanosensation (or mechanotransduction according to other authors [23]) thanks to their capacity to coordinate the regulation of bone mass and structure: indeed, they release biochemical factors that control the activity of both osteoclasts and osteoblasts. Osteoclasts are large, multinucleated giant cells formed from the fusion of mononuclear progenitors and are mainly responsible for bone resorption; osteoblasts derive from mesenchymal stem cells in the bone marrow and are responsible for bone matrix deposition and mineralization [24]. Physiologically, bone remodeling is necessary to repair damaged bone and avoid the effects of aging. Thus, the maintenance of healthy bone is eventually assured by the balanced actions of osteoclasts (resorption) and osteoblasts (deposition), whose orchestrated functions result in the correct bone remodeling (Figure 2).

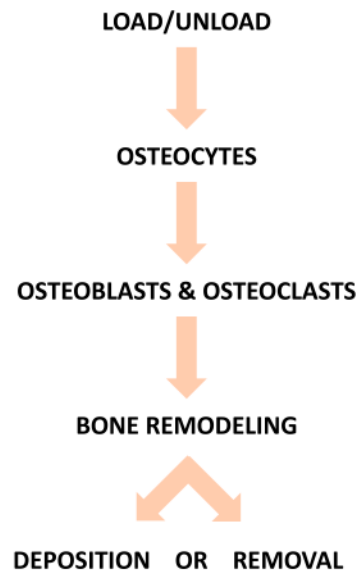


Figure 2. The orchestrated mechanism of mechanosensation.

When the body weight is equally distributed over the lower limbs, the remodeling is properly regulated. Viceversa, when a prosthetic device is introduced into the bone, it significantly modifies the distribution of loads, thus altering the appropriate bone remodeling: in particular, the presence of the hip prosthesis can induce the formation of atrophic bone in the region of the femur that is no longer physiologically loaded (stress protected or stress shielded zone) and denser bone in the area exposed to stresses higher than physiological.

The phenomenon is a direct consequence of the different mechanical properties (stiffness) between the bone tissue and the implanted materials: for example, metals have significantly higher stiffness values than both cortical and spongy bone (Table 1). This gap

causes the stress-shielding effect, exposing the atrophic bone, of poor quality, to possible fractures. This event can be intuitively explained by considering the stem and the femur as an extremely simplified mechanical model composed of two springs in parallel: the one with a higher elastic constant (the metallic stem) will be loaded with a greater amount of external force. In this sense, the magnitude of femoral stress shielding can be estimated using the composite beam theory. This analytical method predicts that the reduction in femoral stress following the implantation of a prosthesis is proportional to the relative structural stiffnesses of bone and femoral stem. Therefore, a stem with a large diameter will cause a more significant bone loss compared to a device with a smaller diameter implanted in the same anatomical site [25]. The study by Engh and Bobyn [26] reported that the incidence of osteolysis following arthroplasty with an uncemented stem increases contextually with the increase in the degree of stress shielding predicted by the compound beam theory. Osteolysis is also related to possible aseptic loosening of the implant [27].

Table 1. Elastic modulus (E, GPa) of some metallic materials used for the production of hip prostheses, compared to cortical and spongy bone.

Material/Tissue	Elastic Modulus E [GPa]
Cortical bone	16
Spongy bone	0.1
316L Stainless Steel	200
Ti6Al4V Alloy	110
CoCr Alloy	230

Mechanical loosening due to the physiological response of the bone, which is dynamic, is one of the main factors negatively affecting an implant's lifespan [28]. In this sense, it has been recognized that the choice of material with superior mechanical characteristics is not always the best solution. When the prosthesis is inserted into the medullary canal of the femur, the load that is normally applied to the proximal portion of the femur is drastically altered, causing bone resorption, bone loss, thinning of the cortical bone, and, in some cases, failure of the prosthesis [28]. By inserting the femoral component of a total hip prosthesis, the stresses on the proximal and medial regions of the femur are reduced, because most of the load bypasses this area and is transmitted from the metal shaft to the distal portion of the femur (Figure 3).

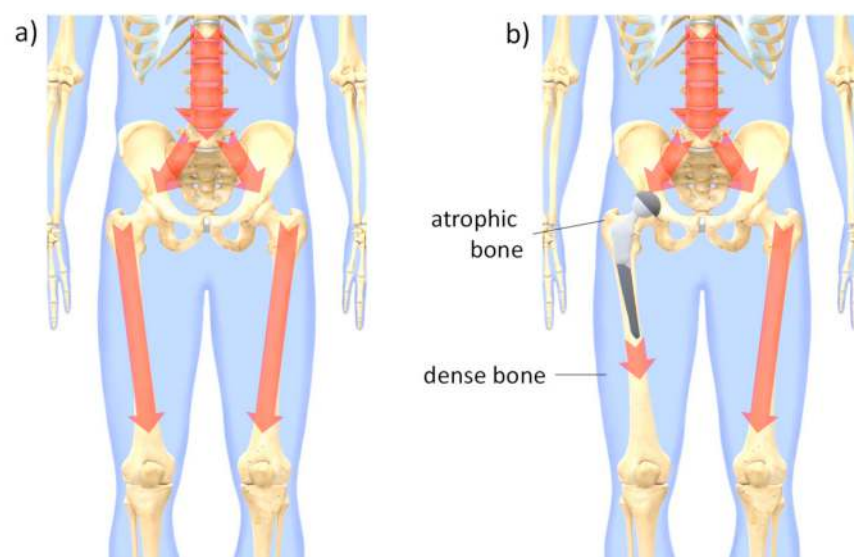


Figure 3. Physiological distribution of the load (a) and altered distribution of the load due to the insertion of a hip prosthesis (b).

Weinans and coworkers defined the stress-shielding as the change in strain energy (SE) in each bone element in which the prosthesis is inserted with respect to a reference value in the intact bone [29]:

$$\text{Stress – shielding signal} = \frac{SE(\text{treated}) - SE(\text{reference})}{SE(\text{reference})}$$

where the deformation energy SE is obtained by dividing the deformation energy density SDE by the apparent density: it is calculated in a formal way analogous to the absolute density, but taking into consideration the total volume occupied by the solid or its external dimensions, therefore including empty spaces, such as solids with closed cavities, with open cavities or with a spongy structure. Other stress-shielding definitions related to stress or strain can be applied equivalently [30].

Thanks to the finite element model proposed by Swanson et al. [31], the stress-shielding effect can be mapped by comparing the distribution of femoral stresses without the prosthetic device with that in the presence of it. Considering 16 points along the medial and lateral sides of the bone (with and without implant), the analysis demonstrated that the bone undergoes a substantial redistribution of the loads following the insertion of the femoral stem. The most evident differences concern the proximal segment of the femur: in the medial proximal sector, physiological compression is drastically reduced.

Following implant insertion, the physiological compressive stress (about 25 MPa) is set to zero in the proximal medial side of the bone. Additionally, in the proximal lateral portion, the traction decreases considerably. These portions are protected from the stress (stress shielded zones), thus atrophic bone is formed. On the other hand, stresses increase in modulus in the areas adjacent to the extremity of the prosthetic stem (e.g., distal femoral portion), overloading this part of the bone. In the medial portion, the tensile load increases, and in the lateral part, the compression becomes more intense: these portions of the femur have to support a load that is higher than physiological. As a consequence, they will be affected by bone hypertrophy, that is the formation of denser bone.

As evidenced by Huiskes in 1993 [32], the choice of the implantation strategy plays an important role: uncemented stems are associated with a more marked stress-shielding effect than the cemented ones. This is due to the fixation method and implant design. Indeed, stems of non-cemented prostheses usually have larger dimensions than cemented ones: consequently, they possess higher stiffness and can adsorb larger loads, resulting in a greater stress-shielding effect. Furthermore, it seems that the bone cement allows a more uniform distribution of the external loads, due to its stiffness that is halfway between that of the stem and the femur, and to the fact that the bone cement fills the gap between the prosthesis and the bone, allowing the maximization of the area of mechanical interface. Femoral stress-shielding is evident in the proximal portion and significantly decreases for both types of anchorage moving towards the distal area.

As reported in [30], the study by Lozynsky et al. demonstrated that in patients with implants aged 12–191 months, the proximal region of the femur exhibits the highest rate of osteolysis, 40% on average. Moreover, femoral stress-shielding, causing the reduction of implant support, significantly increases the risk of mechanical loosening. The effects of the relative micro-mobility of the prosthesis can result in difficulties for patients during daily activities, making prosthetic revision surgery necessary.

Another recent paper investigated the biomechanical variation in overall femoral stress and periprosthetic femoral stress distribution after prosthesis implantation [33]. The authors developed a finite element model of both femur and prosthesis (i.e., the Ribbed model by Ribbed Hip system, Waldemar Link, Hamburg, Germany) and found a significant alteration of stress distribution caused by the presence of the implant. They calculated the stress-shielding ratio as the percent change of the equivalent stress pre and post-surgery in each of the 16 sections examined along the femur. The stress level gradually increased from the proximal to the distal region of the bone.

3. How to Prevent Femoral Stress-Shielding

In order to guarantee the correct distribution of stresses and prevent bone resorption resulting from the stress-shielding effect, several solutions have been developed over the years with specific regard to the femoral component of the hip prosthesis. Alternative designs, coatings, and biomaterials used will be illustrated in the following section.

3.1. Prosthesis (Re)design

Being the stress-shielding phenomenon due to the altered distribution of load because of the presence of the prosthetic system, several efforts have been addressed to redesign the prosthetic device in order to transfer the load to the bone in a more physiological way. An interesting review on the design criteria for hip prosthesis production was published by Joshi et al. [34].

3.1.1. The Short Stem

Hip prostheses with short stems have been developed: the femoral component generally measures less than 120 mm in length (distance from the center of the head to the apex of the stem), allows conservative surgery, and assures a better transmission of the metaphyseal load. However, long-term clinical outcomes are still lacking: thus, the performance of the prosthesis has been evaluated in vitro. The study published by Bieger et al. [35] analyzed the primary stability and the stress-shielding effect associated with a short stem prosthesis (optimys™, Mathys, Bettlach, Switzerland) and a conventional device (CBC™, Mathys) in nine pairs of human cadaveric femurs. The results suggest a more uniform load distribution in the proximal medial portion for the short stem prosthesis, with a stress variation of approximately 47%. On the other hand, the conventional design reveals an altered load of about 80%. In the proximal lateral section, the change is limited (about 6–7%); in the central portion, differences are moderate, especially in the lateral part; in the distal region, differences are significant: the short stem guarantees more uniform distribution of the load with percent differences ranging from approximately 12% for the lateral portion to 7–8% for the medial section. With regard to the micromotions, the authors stated that the short stem displayed lower values at the proximal compared to the distal points, with the opposite findings around the straight stem: this finding suggests a more stable metaphyseal fixation of the short stem and a more diaphyseal anchorage of the straight one. These results have been confirmed by numerical studies, which found a smaller stress-shielding effect in the proximal femur following the implantation of short stems compared to longer stems [36]. Furthermore, some clinical studies on short stems showed a more contained reduction of the mineralized bone matrix, associated with a less marked proximal femoral osteolysis. It is recognized that variations in proximal load transfer depend on the fixation position of the implant; however, the short stem does not guarantee the absence of the phenomenon [36]. It is worthy to notice that the reduction of the stem length can cause reduced stability of the implant, which also depends on soft tissue integrity: this evidence was illustrated by Fetto [37], who developed a comprehensive model to better predict the behavior of the prosthetic system. Anyhow, he found that shorter stems can assure higher levels of stress in the proximal region and the radiographic findings did not show evident changes in the femoral bone mass.

3.1.2. The Hollow Stem

The stiffness of the stem depends on the geometry of its cross-section and on the elastic modulus of the material: it has a crucial influence on the stresses absorbed by the entire prosthetic system and, consequently, on the stress-shielding effect. The results obtained by Gross and Abel [38] showed a reduced proximal stress-shielding effect using stems with hollow sections. Different designs have been compared and some of them provided superior performances at least by finite element analysis. Indeed, the advantage of the hollow configuration lies in the possibility to control stem stiffness through the overall design and the choice of internal diameters. The authors showed that increasing

the internal diameter simultaneously increases the load applied to the bone, both for an external diameter of 10 mm and for one of 11 mm: in the first case, the load progressively increases up to an equivalent von Mises tension of 7.28 MPa, increasing the proximal stress value by 18.37% compared to the solid stem. The result is even better in the case of an external diameter of 11 mm, with an increase in proximal stress of 28.21% in the case of a stem with an internal diameter of 9 mm. They also suggested that the external shape of the stem can be defined on the basis of a single patient's anatomical requirements.

3.1.3. The Ribbed Stem

The study by Wu et al. [39] evaluated the effects of the Ribbed anatomic cementless femoral stem on bone remodeling and bone mineral density (BMD) in 41 patients (19 males and 22 females, average age 62.07 years). The short and medium-term follow-up of patients who received the grooved stem prosthesis (Ribbed Hip system), pointed out restrained osteolysis in the proximal areas of the femur. BMD of the seven Gruen zones (Figure 4) was measured by dual-energy X-ray absorptiometry, and contact, fitness, and fixation of the femoral stem and proximal femur were analyzed by X-ray [40]. Compared with the contralateral unoperated side, significant reductions of periprosthetic BMD were detected in the Gruen zones 4 and 5 on the prosthetic side. Other significant differences were not detected. Authors concluded that BMD changes imply that more proximal stress is distributed in the proximal lateral region (Gruen zone 1: +5.542%) and middle medial zone (Gruen zone 6: +1.617%), accompanied with evident stress-shielding in the distal zone (Gruen zone 4: −5.799%) and medial distal zone (Gruen zone 5: −2.845%).

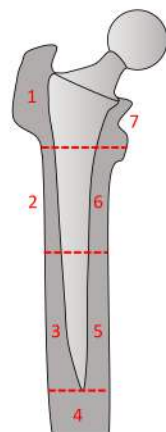


Figure 4. The Gruen zones (marked from 1 to 7) are conventionally used to identify the areas of the prosthetic system where bone remodeling has to be assessed [40].

The results of the finite element analysis published by Luo et al. [33] showed that the area mainly affected by the stress-shielding effect is the posterior region of the femur (authors adopted a mapping criterium different from the Gruen zones). Due to the porous coating of the proximal section of the Ribbed prosthesis, the problem of the stress-shielding caused by the concentration of stresses in the medial and distal regions was solved. The study also stated that the deep grooves on the stem surface reduce its cross-section and provide a “constructive elasticity” which, combined with the mechanical properties of titanium, reduces the proximal stress-shielding phenomenon.

3.2. Surface Treatment and Coating

Several attempts to promote the fixation of the stem to the femur have been investigated and implemented, with specific regard to the treatment of the prosthetic surface. Two kinds of cementless prostheses have been developed: those promoting bone growth on the surface of the prosthetic stem itself (ongrowth) and those promoting bone growth within a microscopic three-dimensional structure that coats the body of the prosthesis (ingrowth).

3.2.1. Ongrowth Anchoring

To promote the anchorage of the prosthetic stem to the bone by ongrowth, surface modifications are applied: they allow retaining the desired bulk properties of the stem while modifying the external surface, which is directly in contact with the biological tissue. Surface modifications can be achieved by several approaches [41,42]. In particular, two techniques are usually employed: sandblasting and plasma spray. Sandblasting requires abrasive particles (e.g., alumina, corundum, rutile) to be dragged into a pressurized fluid against the surface: the impact of the particles increases surface roughness, which value mainly depends on particles size and treatment duration [42,43].

Hydroxyapatite (HA) coating is a particular type of plasma spray technique [44]. HA is a phosphocalcic ceramic and represents the main mineral component of the bone tissue matrix. HA coatings are acknowledged to offer some advantages: they stimulate bone formation, accelerate implant fixation to bone, reduce the risk of release of metallic wear particles or metallic ions from implants [45]. Once a strong osteo-apposition is achieved, HA gradually disappears due to bone remodeling: therefore, the HA coating is replaced by newly grown bone. HA has been widely applied to coat metallic stems and it is recently proposed also to coat composite stems (see CF/PA composite).

Clinical studies have shown that fully HA-coated stems are associated with greater stress-shielding than those coated only in the proximal region [46]. Currently, the amount of coating on most prosthetic stems is still inadequate to reduce the proximal stress-shielding effect. However, the reduction of the porous coating has to be balanced with the amount of coating necessary to ensure a solid implant fixation.

3.2.2. Ingrowth Anchoring

The fixation of the prosthesis by bone ingrowth is based on the ability of bone cells to populate the pores present on the stem surface. Scientific evidence have shown that an optimal bone ingrowth requires a pore diameter ranging between 100 and 400 μm [47]. Various technical solutions have been adopted to create these kinds of pores, including sintered metal microspheres over the prosthetic stems, micro-meshes made of metal fiber, and porous metals. Moreover, a porous structure allows reducing the stiffness of the implant, an effective way to relieve femoral stress-shielding [48].

Porous metal implants ensure a more uniform stress distribution than smoothed ones and allow greater long-term stability. However, it is worthy to consider that an excessive reduction of stiffness can cause relative micro-movements between the implant and the patient's bone; excessive micro-movements can hamper the formation of newly grown bone tissue, preventing the adhesion of bone cells to the implant surface.

Wang et al. demonstrated that the lower stiffness of porous femoral stems increases load transfer to the proximal femur compared to fully dense femoral stems [49]: the introduction of porosity into the femoral stem design can alleviate the problem of stress-shielding around the prosthesis. In particular, in the case of fully dense stems, the total volume of bone with decreased density is almost 75% higher than that of porous stems: this outcome explains the advantages of low-stiffness implants compared to high stiffness ones. However, compared to dense titanium, porous titanium has a lower fatigue resistance with a higher risk of fracture or long-term failure. Therefore, the problem of femoral stem fatigue should not be ignored, especially for porous stems.

3.3. Innovative Biomaterials

Manufacturers of prosthetic devices have been progressively moving towards the exploitation of biomaterials with mechanical features replicating those of the bone tissue rather than superior. The mechanical resistance of the stem depends on its thickness and on its elastic modulus (stiffness).

A clear relation between the mechanical characteristics of the prosthetic stem and peri-implant bone resorption had been illustrated by Huiskes, Weinans, and Van Rietbergen [50]: working on embalmed femurs, these authors simulated and compared the effects caused

by the presence of titanium stems ($E = 1.1 \times 10^5$ MPa) and stems made of flexible, isoelastic materials ($E = 0.2 \times 10^5$ MPa, $E = 0.5 \times 10^5$ MPa, $E = 0.8 \times 10^5$ MPa). A 10% increase in stem thickness produces a 33% increase in stem flexural strength. By reducing the longitudinal elastic modulus by a factor of 5.5 (using an elastic material with Young's modulus similar to that of cortical bone), long-term bone loss is considerably reduced, from 23% to 9% [50].

3.3.1. Porous Titanium

In the paper by Arabnejad et al. [51], a high-strength femoral stem was entirely made of porous titanium, whose mechanical properties were adjusted by varying the porosity. The macroscopic design of the implant was based on the short stem concept, which is compatible with minimally invasive surgery; the microarchitecture of the implant was optimized by means of computational methods in order to locally emulate the properties of the bone tissue and minimize the stress-shielding effect. Bone was considered isotropic material: indeed, this simplification did not involve significant differences with respect to the results obtained by considering bone as an orthotropic material. Once the optimal density distribution was obtained, the stem was produced by selective laser melting (SLM), an additive manufacturing technique using high power-density laser to melt and fuse metallic powders. Porosity and pore size was set at 70% and 500 μm , respectively. Bone resorption was assessed by the Digital Image Correlation (DIC) test comparing the porous stem with a commercially available implant of identical but solid geometry. The physiological FEA model shows that the total bone loss due to the stress-shielding effect for the traditional stem was 34%, concentrated in the proximal medial portion (Gruen zone 7). For the porous implant, the bone loss was only localized in the proximal medial portion (8%). This outcome suggests that osteolysis in a completely porous implant is 75% lower than in a traditional one. Furthermore, the bone loss was confined to a single Gruen region. Moreover, with regard to the Gruen zone 6, the volumetric bone loss was reduced by 86% as shown in the FEA corresponding to the quasi-physiological DIC experiment. In general, for the porous implant, the stress-shielding effects were considerably limited compared to a traditional implant.

3.3.2. β . Ti–33.6Nb–4Sn Alloy

Many attempts have been exploited in order to improve the mechanical features of the materials used for manufacturing the hip prosthesis components. For example, elements such as iron and niobium have been added to titanium-aluminum alloys to get higher dynamic stiffness and lower elastic modulus. Therefore, Ti5Al2.5Fe and Ti6Al7Nb alloys allow a better distribution of stress between the implant and bone tissue and a lower elastic modulus.

Another class of titanium alloys (β -Ti alloys) exploited for orthopedic applications contains molybdenum: its presence stabilizes the titanium β phase at room temperature. In 2014, Hanada et al. [52] were the first to develop a new cementless stem with Young's modulus decreasing from the proximal to the distal area using the new β -Ti-33.6Nb4Sn alloy (TNS). The longitudinal elastic modulus and the strength of this alloy depend on the temperature at which the heat treatment is carried out. A local heat treatment (693 K for 5 h in N_2 atmosphere) applied in the proximal region, increases the resistance of the prosthetic neck compared to the Ti6Al4V alloy.

TNS stems were evaluated in a multicenter, open-label, single-arm clinical trial published by Chiba et al. [53]. The results of 3-years follow-up on 40 patients were assessed and revealed no radiologic signs of loosening, subsidence, or breakage of the stem. Indeed, this study presents some limitations (no control group, few patients, short follow-up): nevertheless, it confirmed that TNS alloy is suitable for the production of the stem component of a total hip prosthesis with a mild stress-shielding effect on 65% of patients.

The work of Yamako et al. [54] demonstrated that a TNS stem causes bone resorption lower than a Ti6Al4V one in almost all the Gruen areas. Bone loss occurred mainly in the proximal part of the femur (Gruen zones 1, 6, and 7). The difference in BMD between the

two stems gradually increased over time in the proximal regions. Specifically, in Gruen zone 7, the difference in BMD was by 4.6% at 2 years (Ti6Al4V stem: 81.8%; TNS stem: 86.4%), 10.8% at 5 years (Ti6Al4V stem: 60.2%; TNS stem: 71.0%), and 16.2% at 10 years (Ti6Al4V stem: 38.0%; TNS stem: 54.2%). In this region, the TNS alloy stem ensured a reduction in bone density lower than the traditional titanium alloy stem. The FE simulation showed that the stresses transmitted to the bone in the proximal medial region in the immediate postoperative period are 18% higher with the TNS stem than with the Ti6Al4V stem. This indicates a greater proximal load with the TNS stem. Similar results had been obtained in a previous in vitro experimental study [55]. The stresses transmitted in the above-mentioned region for the TNS stem were consistently greater than for the traditional titanium alloy stem. Indeed, the authors concluded that proximal femoral bone loss due to the stress-shielding phenomenon was not completely eliminated; nevertheless, the TNS stem with a gradual variation of Young's modulus demonstrated advantageous effects on bone preservation and ensured sufficient mechanical resistance.

3.3.3. CF/PEEK Composites

It has been shown that the properties of carbon fiber reinforced polyetheretherketone—PEEK (Carbon/PEEK or Carbon Fiber PEEK or CF/PEEK) are very close to those of human bones and significantly different from those of other materials used for the manufacture of the hip prosthesis [56,57]. CF/PEEK composites can ensure a more uniform transfer of loads from implant to bone, thus limiting the stress-shielding effect. The mechanical properties of these materials vary accordingly with the orientation of the carbon fibers and their overall fraction in the composite (strength ranging from 70 to 1900 MPa and stiffness between 10 and 100 GPa). In addition, the CF/PEEK composites have shown excellent biocompatibility, environmental stability, and chemical resistance. It is worthy to add that these materials can be produced with different arrangements of carbon fibers within the PEEK matrix: this can be the way to adjust the elastic modulus along the stem to reduce the stress-shielding effect.

In the study by Carpenter et al. [58], a porous PEEK implant was compared with a porous titanium one. The results confirmed that the former significantly increased the transfer of load to the bone compared to porous Ti under compression (PEEK = 66%; Ti = 13%), traction (PEEK = 71%; Ti = 12%) and shear (PEEK = 68%; Ti = 9%) evaluated over a 4-week period. The extent of the stresses transmitted to the bone increased, on average, by 83%. The application of the mechanical properties of PEEK to the geometry of the Ti implant, and vice versa, demonstrated that the increase in load sharing with bone was mainly due to differences in the intrinsic elastic modulus of the materials rather than to the architecture of the pores.

The study by Anguiano-Sanchez et al. [59] demonstrated that a PEEK coating applied to a hip prosthesis improves the distribution of stresses in the proximal area, decreasing the stress-shielding phenomenon and increasing the lifespan of the implant. The PEEK coating proposed in the study shows a 47% increase in load transfer in the proximal area with a 100 µm thick coating; increasing the thickness up to 400 µm, the stress transmission improves by 60%.

Another recent paper investigated the application of PEEK and CF/PEEK composite (with different fibers orientations) as coating materials [60]: the analysis was carried out by the finite element method and demonstrated that both safety and durability of the prosthetic system are enhanced by CF/PEEK coating (with multidirectional orientation). This coating material is able to distribute the applied load to the bone minimizing the stress-shielding effect.

Nakahara et al. [61] investigated the radiographic and histological results for cementless or cemented CF/PEEK hip prostheses implantation in an ovine model. After 52 weeks, five cementless and four cemented cases showed 1st-degree stress-shielding and two cemented cases showed 2nd-degree stress-shielding; 3rd-degree stress-shielding

was not observed at all and this evidence suggested that the load is transferred in a more physiological way from the stem to the femur without stress concentration.

3.3.4. CF/PA 12 Composite

Other carbon fiber reinforced polymer composites have been shown as very promising biomimetic materials for orthopedic applications. In particular, the study by Tavakkoli et al. [62] investigated the CF/PA 12 composite: this material is obtained by reinforcing a nylon 12 matrix with carbon fibers. The properties of this composite material were compared with titanium and CoCrMo alloys. Post-operative bone density and bone loss were assessed by FEA. Authors found that the implant made with CoCrMo alloy, being the most rigid one, induced considerable stress-shielding (predominant bone density between 0.34–0.8 g/m³); on the other hand, the biomimetic CF/PA 12 material ensured a more homogeneous transmission of loads in the proximal region and consequently reduced the amount of bone reabsorption after implantation. Experimental data collected with regard to the Gruen zones confirmed that the biomimetic composite can assure an amount of bone loss of 9%: this value is significantly lower than CoCrMo (27%) and Ti6Al4V (21%) alloys. In particular, the Gruen zone 7 recorded the most significant bone loss for metal alloys, in agreement with the literature: 43% for CoCrMo and 35% for titanium alloy. In the same portion, CF/PA 12 showed a bone loss of about 9%. Moreover, standard deviation values of about 0.6% for the composite material confirm a much more uniform load distribution compared to metal alloys ($\sigma = 9.13\%$ for titanium alloy and $\sigma = 12.29\%$ for CoCrMo). Taken together, the results of this study suggest that, in terms of bone remodeling, the prosthetic implant made of CF/PA 12 showed significant advantages over metal alloys, ensuring lower stress-shielding effects and more contained and homogeneous changes in bone density.

4. Other Design Solutions

Recently, lattice and cellular structures have attracted the attention of many researchers from different fields, from bioengineering to aerospace engineering. Thanks to the possibility to optimize the geometric distributions of strut size, pore morphology, and macroscopic apparent density, these structures can be suitable for improving bone regeneration and controlling the mechanical stimulus transferred from implant to bone [63]. Their fabrication requires non-traditional technologies (Figure 5): among the others, additive manufacturing allows achieving the precise fabrication and the tunable mechanical features of lattice structures with complicated topologies [64].

Surface treatments	<ul style="list-style-type: none"> • Chemical and physical deposition • Thermal spray • Chemical modification • Plasma spray • Electrode/ion beam assisted deposition
Bulk treatments	<ul style="list-style-type: none"> • Casting • Sedimentation • Solidification • Powder metallurgy • Sintering • Photopolymerization • Extrusion • Lamination • Powder bed fusion • Binder jetting • Material jetting

Figure 5. Examples of technologies for functionally graded materials (FGMs) production.

The term “functionally graded materials (FGMs)” has been proposed to indicate “advanced engineering materials designed for a specific performance or function in which a spatial gradation in structure and/or composition lend itself to tailored properties” [65]. Indeed, FGMs include a variety of materials, from ceramics to metals, from polymers to

composites. Generally speaking, FGMs try to mimic natural structures because these natural components have excellent features with respect to their specific application, whereas manmade parts are still far from them [66].

FGMs are emerging materials for orthopedic applications [66]: the gradual variation of their properties in space can reproduce the local properties of the native bone, minimizing the stress-shielding effect [67], at the same time reducing the shear stress between the implant and the surrounding bone tissue.

With specific regard to the reduction of the stress-shielding effect, Mustafa G. Gok created and analyzed multi-lattice structures for the design of a hip stem implant made of Ti6Al4V [68]. The proximal part of the stem was divided into three regions: simple cubic, body-centered cubic, and face-centered cubic lattice structures were created on the upper part. These multi-lattice designs caused a reduction of the maximum von Mises stress values on the prosthetic stem (from 289 to 189 Mpa), in parallel with a reduction of the weight (−25.89%). Stress-shielding signals were obtained by determining the change in strain energy per unit bone mass caused by the presence of the femoral hip implant stem and its ratio to the intact bone. In the case of hip-stems with multi-lattice designs, there was a significant increase (max. 150.47%) in stress-shielding signals from different zones of the femur: the stress-shielding effect was significantly reduced thanks to multi-lattice designs.

In general, two categories of cellular structures are considered: stochastic and non-stochastic. The first ones are characterized by random variations in the shape and size of the cells; the second ones by the regular repetition of lattice structures [69].

Many are the papers published on both the structural characterization and the mechanical properties of FGMs, some of them regard the possibility to produce custom-made implants according to the data acquired from the patient via computed tomography (CT). CT scan, along with a microstructural examination and mechanical testing, also allowed comparing various geometrical arrays of cellular, reticulated mesh, and open-cell foams with interconnected porosities for the production of the so-called “next-generation” biomedical implants: the variable density/porosity results in an optimized matching between the mechanical properties of the implant and the bone to reduce/eliminate the risks associated with the stress-shielding effect [70]. Other papers that are worth mentioning are: the FE analysis by Oshkour et al. [71], who developed a three-dimensional model of femoral stem made of FGM to successfully decrease the stress-shielding area; the work published by Ahirwar et al. [72], who compared the performances (in terms of stress distribution) of Ti-HA, CoCr-HA and SS316L-HA prostheses observing a more favorable behavior of the first one with respect to the others; the study by Al-Jassir et al. [73], who computationally explored von Mises stresses at the interface between bone cement and stem: they decreased significantly when using FG material instead of CoCrMo and Ti alloy; the work published by Chowdhury et al. [74] on the superior mechanical properties of porous Ti-Nb alloy for orthopedic applications due to the lower elastic modulus and higher biocompatibility; the numerical analysis combined with physical testing by Hazlehurst, Wang and Stanford [75], who proposed a CoCrMo stem with graded porous structure able to reduce the risk of implant loosening because of the stress-shielding effect, while maintaining bone-implant interface stability.

5. Conclusions and Future Perspectives

An exhaustive review on materials development, design strategies, and manufacturing technologies for the production of total hip prostheses able to minimize the stress-shielding phenomenon are necessarily outside the scope of the present work. Indeed, the reviewed papers are extremely heterogenous: they cover a wide range of topics from FE simulations to in vivo studies, from metallic components (Ti, Ti alloys, CoCrMo, stainless steel, ...) to reinforced composites, from cemented and cementless stems to clinical trials. Being so diverse, it is hard to compare these papers with each other. Anyhow, we can state that, on the one hand, the stress-shielding phenomenon has been deeply characterized and understood; on the other hand, this phenomenon can be reduced but not completely

circumvented. For sure, the recently proposed patient-specific approaches for designing and manufacturing tailored prosthetic systems can consider the individual characteristics of every single patient to provide them with the optimal implant solution [76,77].

In this perspective, it appears more and more evident that clinical and surgical competencies have to be technically supported by the contribution of the “engineering community”: mechanical engineers, materials engineers, bioengineers, computer science engineers, together they have to “create” a customized prosthetic device from patient’s CT or NMR images [78,79]. Currently available technical instrumentations and computational resources allow extending this approach and translating it into clinical practice.

As highlighted by Fontalis et al. [80], patient-specific instrumentation (PCI) not only permits us to create customized devices, for example, by means of 3D printing technologies that can replicate the anatomy of the surgical site and the mechanical and structural characteristics of the bone and the prosthesis. This approach has limitless applications in orthopedic surgery: it is currently restrained by the high costs and the lack of regulatory requirements. Moreover, an extremely accurate pre-operative planning can be performed through new technologies like virtual reality (VR): it represents a very powerful tool to simulate the “real” surgery, allowing surgeons to train themselves in a “virtual” operating room on a “virtual” patient, who replicates the “real” one [81,82]. Recent technological advances also offer computer navigation systems and robotic-assisted surgery to guide the position of the cutting blocks and to perform the cut, respectively [83].

Taken together, these tools can generate a fundamental contribution in improving the precision of the surgical act and improve the match between patient’s anatomy and prosthetic device to reduce the stress shielding effect [84]. Finally, it is worthy to mention the “ultimate goal” of hip arthroplasty: “generating a reproducible, durable, “forgotten” prosthetic hip” [83].

Author Contributions: Conceptualization, D.S. and A.B.; methodology, D.S. and A.B.; data curation, D.S. and A.B.; writing—original draft preparation, D.S. and A.B. writing—review and editing, D.S. and A.B.; visualization, A.B.; supervision, A.B. All authors have read and agreed to the published version of the manuscript.

Funding: This research received no external funding.

Conflicts of Interest: The authors declare no conflict of interest.

References

1. Knight, S.R.; Aujla, R.; Biswas, S.P. Total Hip Arthroplasty—Over 100 years of operative history. *Orthop. Rev.* **2011**, *3*, e16. [CrossRef] [PubMed]
2. Sershon, R.; Balkissoon, R.; Valle, C.J. Current indications for hip resurfacing arthroplasty in 2016. *Curr. Rev. Musculoskelet. Med.* **2016**, *9*, 84–92. [CrossRef] [PubMed]
3. Gomez, P.F.; Morcuende, J.A. Early attempts at hip arthroplasty—1700s to 1950s. *Iowa Orthop. J.* **2005**, *25*, 25–29. [PubMed]
4. Charnley, J. Arthroplasty of the hip. A new operation. *Lancet* **1961**, *1*, 1129–1132. [CrossRef]
5. Hip and Knee Replacement. Available online: <https://www.oecd-ilibrary.org/sites/2fc83b9a-en/index.html?itemId=/content/component/2fc83b9a-en> (accessed on 13 March 2022).
6. Singh, J.A.; Yu, S.; Chen, L.; Cleveland, J.D. Rates of total joint replacement in the United States: Future projections to 2020–2040 using the National Inpatient Sample. *J. Rheumatol.* **2019**, *46*, 1134–1140. [CrossRef]
7. Lee, J.M. The Current Concepts of Total Hip Arthroplasty. *Hip Pelvis* **2016**, *28*, 191–200. [CrossRef]
8. Siopack, J.S.; Jergesen, H.E. Total hip arthroplasty. *West. J. Med.* **1995**, *162*, 243–249.
9. Petis, S.; Howard, J.L.; Lanting, B.L.; Vasarhelyi, E.M. Surgical approach in primary total hip arthroplasty: Anatomy, technique and clinical outcomes. *Can. J. Surg.* **2015**, *58*, 128–139. [CrossRef]
10. Enge, J.D.J.; Castro, A.A.; Fonseca, E.K.U.N.; Baptista, E.; Padial, M.B.; Rosenberg, L.A. Main complications of hip arthroplasty: Pictorial essay. *Radiol. Bras.* **2020**, *53*, 56–62. [CrossRef]
11. Del Pozo, J.L.; Patel, R. Clinical practice. Infection associated with prosthetic joints. *N. Engl. J. Med.* **2009**, *361*, 787–794. [CrossRef]
12. Tavakkoli Avval, P.; Klika, V.; Bougherara, H. Predicting bone remodeling in response to total hip arthroplasty: Computational study using mechanobiochemical model. *J. Biomech. Eng.* **2014**, *136*, 051002. [CrossRef]
13. Sharma, R.; Vittal, V.K.; Gupta, V. Homogeneous modelling and analysis of hip prosthesis using FEA. *J. Phys. Conf. Ser.* **2019**, *1240*, 012118. [CrossRef]

14. Joshi, T.; Sharma, R.; Mittal, V.K.; Gupta, V.; Krishan, G. Dynamic analysis of hip prosthesis using different biocompatible alloys. *Open J. Eng. ASME* **2022**, *1*, 011001. [\[CrossRef\]](#)
15. Brodt, S.; Matziolis, G.; Buckwitz, B.; Zippelius, T.; Strube, P.; Roth, A. Long-term follow-up of bone remodelling after cementless hip arthroplasty using different stems. *Sci. Rep.* **2020**, *10*, 10143. [\[CrossRef\]](#) [\[PubMed\]](#)
16. Stukenborg-Colsman, C.M.; von der Haar-Tran, A.; Windhagen, H.; Bouguecha, A.; Wefstaedt, P.; Lerch, M. Bone remodelling around a cementless straight THA stem: A prospective dual-energy X-ray absorptiometry study. *Hip Int.* **2012**, *22*, 166–171. [\[CrossRef\]](#) [\[PubMed\]](#)
17. Sluimer, J.C.; Hoefnagels, N.H.; Emans, P.J.; Kuijer, R.; Geesink, R.G. Comparison of two hydroxyapatite-coated femoral stems: Clinical, functional, and bone densitometry evaluation of patients randomized to a regular or modified hydroxyapatite-coated stem aimed at proximal fixation. *J. Arthroplast.* **2006**, *21*, 344–352. [\[CrossRef\]](#) [\[PubMed\]](#)
18. Jahnke, A.; Wiesmair, A.K.; Fonseca Ulloa, C.A.; Ahmed, G.A.; Rickert, M.; Ishaque, B.A. Outcome of short- to medium-term migration analysis of a cementless short stem total hip arthroplasty using EBRA-FCA: A radiological and clinical study. *Arch. Orthop. Trauma Surg.* **2020**, *140*, 247–253. [\[CrossRef\]](#)
19. Morita, A.; Kobayashi, N.; Choe, H.; Tezuka, T.; Hiashihira, S.; Inaba, Y. Preoperative factors predicting the severity of BMD loss around the implant after Total hip Arthroplasty. *BMC Musculoskelet. Disord.* **2021**, *22*, 290. [\[CrossRef\]](#)
20. Frost, H.M. Wolff's Law and bone's structural adaptations to mechanical usage: An overview for clinicians. *Angle Orthod.* **1994**, *64*, 175–188. [\[CrossRef\]](#)
21. Oftadeh, R.; Perez-Viloria, M.; Villa-Camacho, J.C.; Vaziri, A.; Nazarian, A. Biomechanics and mechanobiology of trabecular bone: A review. *J. Biomech. Eng.* **2015**, *137*, 0108021–01080215. [\[CrossRef\]](#)
22. Klein-Nulend, J.; Bakker, A.D.; Bacabac, R.G.; Vatsa, A.; Weinbaum, S. Mechanosensation and transduction in osteocytes. *Bone* **2013**, *54*, 182–190. [\[CrossRef\]](#) [\[PubMed\]](#)
23. Yavropoulou, M.P.; Yovos, J.G. The molecular basis of bone mechanotransduction. *J. Musculoskelet. Neuronal Interact.* **2016**, *16*, 221–236. [\[PubMed\]](#)
24. Siddiqui, J.A.; Partridge, N.C. Physiological Bone Remodeling: Systemic Regulation and Growth Factor Involvement. *Physiology* **2016**, *31*, 233–245. [\[CrossRef\]](#) [\[PubMed\]](#)
25. Silva, M.J.; Reed, K.L.; Robertson, D.D.; Bragdon, C.; Harris, W.H.; Maloney, W.J. Reduced bone stress as predicted by composite beam theory correlates with cortical bone loss following cemented total hip arthroplasty. *J. Orthop. Res.* **1999**, *17*, 525–531. [\[CrossRef\]](#) [\[PubMed\]](#)
26. Engh, C.A.; Bobyn, J.D. The influence of stem size and extent of porous coating on femoral bone resorption after primary cementless hip arthroplasty. *Clin. Orthop. Relat. Res.* **1988**, *231*, 7–28. [\[CrossRef\]](#)
27. Sumner, D.R. Long-term implant fixation and stress-shielding in total hip replacement. *J. Biomech.* **2015**, *48*, 797–800. [\[CrossRef\]](#)
28. Ait Moussa, A.; Fischer, J.; Yadav, R.; Khandaker, M. Minimizing Stress-shielding and cement damage in cemented femoral component of a hip prosthesis through computational design optimization. *Adv. Orthop.* **2017**, *2017*, 8437956. [\[CrossRef\]](#)
29. Weinans, H.; Sumner, D.R.; Igloria, R.; Natarajan, R.N. Sensitivity of periprosthetic stress-shielding to load and the bone density-modulus relationship in subject-specific finite element models. *J. Biomech.* **2000**, *33*, 809–817. [\[CrossRef\]](#)
30. Ridzwan, M.I.Z.; Shuib, S.; Hassan, A.Y.; Shokri, A.A.; Mohamad Ibrahim, M.N. Problem of Stress-shielding and Improvement to the Hip Implant Designs: A Review. *J. Med. Sci.* **2007**, *7*, 460–467. [\[CrossRef\]](#)
31. Swanson, S.A.V. Mechanical Aspects of Fixation. In *The Scientific Basis of Joint Replacement*; Swanson, S.A.V., Freeman, M.A.R., Eds.; Pitman Medical Publishers: Turnbridge Wells, UK, 1977; pp. 130–157.
32. Huiskes, R. Stress-shielding and bone resorption in THA: Clinical versus computer-simulation studies. *Acta Orthop. Belg.* **1993**, *59* (Suppl. S1), 118–129.
33. Luo, C.; Wu, X.D.; Wan, Y.; Liao, J.; Cheng, Q.; Tian, M.; Bai, Z.; Huang, W. Femoral Stress Changes after Total Hip Arthroplasty with the Ribbed Prosthesis: A Finite Element Analysis. *Biomed. Res. Int.* **2020**, *23*, 6783936. [\[CrossRef\]](#) [\[PubMed\]](#)
34. Joshi, M.G.; Advani, S.G.; Miller, F.; Santare, M.H. Analysis of a femoral hip prosthesis designed to reduce stress-shielding. *J. Biomech.* **2000**, *33*, 1655–1662. [\[CrossRef\]](#)
35. Bieger, R.; Ignatius, A.; Reichel, H.; Dürselen, L. Biomechanics of a short stem: In vitro primary stability and stress-shielding of a conservative cementless hip stem. *J. Orthop. Res.* **2013**, *31*, 1180–1186. [\[CrossRef\]](#) [\[PubMed\]](#)
36. Gómez-Vallejo, J.; Roces-García, J.; Moreta, J.; Donaire-Hoyas, D.; Gayoso, Ó.; Marqués-López, F.; Albareda, J. Biomechanical behavior of an hydroxyapatite-coated traditional hip stem and a short one of similar design: Comparative study using finite element analysis. *Arthroplast. Today* **2021**, *7*, 167–176. [\[CrossRef\]](#)
37. Fetto, J.F. A Dynamic Model of Hip Joint Biomechanics: The Contribution of Soft Tissues. *Adv. Orthop.* **2019**, *4*, 5804642. [\[CrossRef\]](#)
38. Gross, S.; Abel, E.W. A finite element analysis of hollow stemmed hip prostheses as a means of reducing stress-shielding of the femur. *J. Biomech.* **2001**, *34*, 995–1003. [\[CrossRef\]](#)
39. Wu, X.D.; Tian, M.; He, Y.; Chen, H.; Chen, Y.; Mishra, R.; Liu, W.; Huang, W. Short to Midterm Follow-Up of Periprosthetic Bone Mineral Density after Total Hip Arthroplasty with the Ribbed Anatomic Stem. *Biomed. Res. Int.* **2019**, *27*, 3085258. [\[CrossRef\]](#)
40. Gruen, T.A.; McNeice, G.M.; Amstutz, H.C. "Modes of failure" of cemented stem-type femoral components: A radiographic analysis of loosening. *Clin. Orthop. Relat. Res.* **1979**, *141*, 17–27. [\[CrossRef\]](#)
41. Lappalainen, R.; Santavirta, S.S. Potential of coatings in total hip replacement. *Clin. Orthop. Relat. Res.* **2005**, *430*, 72–79. [\[CrossRef\]](#)

42. Bagno, A.; Di Bello, C. Surface treatments and roughness properties of Ti-based biomaterials. *J. Mater. Sci. Mater. Med.* **2004**, *15*, 935–949. [[CrossRef](#)]
43. Thomas, K.A. Hydroxyapatite coatings. *Orthopedics* **1994**, *17*, 267–278. [[CrossRef](#)] [[PubMed](#)]
44. Arcos, D.; Vallet-Regí, M. Substituted hydroxyapatite coatings of bone implants. *J. Mater. Chem. B* **2020**, *8*, 1781–1800. [[CrossRef](#)] [[PubMed](#)]
45. Auclair-Daigle, C.; Bureau, M.N.; Legoux, J.G.; Yahia, L. Bioactive hydroxyapatite coatings on polymer composites for orthopedic implants. *J. Biomed. Mater. Res. A* **2005**, *73*, 398–408. [[CrossRef](#)]
46. MacDonald, S.J.; Rosenzweig, S.; Guerin, J.S.; McCalden, R.W.; Bohm, E.R.; Bourne, R.B.; Rorabeck, C.H.; Barrack, R.L. Proximally versus fully porous-coated femoral stems: A multicenter randomized trial. *Clin. Orthop. Relat. Res.* **2010**, *468*, 424–432. [[CrossRef](#)]
47. Abbasi, N.; Hamlet, S.; Love, R.M.; Nguyen, N.-T. Porous scaffolds for bone regeneration. *J. Sci. Adv. Mater. Devices* **2020**, *5*, 1–9. [[CrossRef](#)]
48. Mour, M.; Das, D.; Winkler, T.; Hoenig, E.; Mielke, G.; Morlock, M.M.; Schilling, A.F. Advances in porous biomaterials for dental and orthopaedic applications. *Materials* **2010**, *3*, 2947–2974. [[CrossRef](#)]
49. Wang, S.; Zhou, X.; Liu, L.; Shi, Z.; Hao, Y. On the design and properties of porous femoral stems with adjustable stiffness gradient. *Med. Eng. Phys.* **2020**, *81*, 30–38. [[CrossRef](#)]
50. Huiskes, R.; Weinans, H.; van Rietbergen, B. The relationship between stress-shielding and bone resorption around total hip stems and the effects of flexible materials. *Clin. Orthop. Relat. Res.* **1992**, *274*, 124–134. [[CrossRef](#)]
51. Arabnejad, S.; Johnston, B.; Tanzer, M.; Pasini, D. Fully porous 3D printed titanium femoral stem to reduce stress-shielding following total hip arthroplasty. *J. Orthop. Res.* **2017**, *35*, 1774–1783. [[CrossRef](#)]
52. Hanada, S.; Masahashi, N.; Jung, T.K.; Yamada, N.; Yamako, G.; Itoi, E. Fabrication of a high-performance hip prosthetic stem using β Ti-33.6Nb-4Sn. *J. Mech. Behav. Biomed. Mater.* **2014**, *30*, 140–149. [[CrossRef](#)]
53. Chiba, D.; Yamada, N.; Mori, Y.; Oyama, M.; Ohtsu, S.; Kuwahara, Y.; Baba, K.; Tanaka, H.; Aizawa, T.; Hanada, S.; et al. Mid-term results of a new femoral prosthesis using Ti-Nb-Sn alloy with low Young's modulus. *BMC Musculoskelet. Disord.* **2021**, *22*, 987. [[CrossRef](#)] [[PubMed](#)]
54. Yamako, G.; Janssen, D.; Hanada, S.; Anijs, T.; Ochiai, K.; Totoribe, K.; Chosa, E.; Verdonshot, N. Improving stress-shielding following total hip arthroplasty by using a femoral stem made of β type Ti-33.6Nb-4Sn with a Young's modulus gradation. *J. Biomech.* **2017**, *63*, 135–143. [[CrossRef](#)] [[PubMed](#)]
55. Yamako, G.; Chosa, E.; Totoribe, K.; Hanada, S.; Masahashi, N.; Yamada, N.; Itoi, E. In-vitro biomechanical evaluation of stress-shielding and initial stability of a low-modulus hip stem made of β type Ti-33.6Nb-4Sn alloy. *Med. Eng. Phys.* **2014**, *36*, 1665–1671. [[CrossRef](#)] [[PubMed](#)]
56. Ma, H.; Suonan, A.; Zhou, J.; Yuan, Q.; Liu, L.; Zhao, X.; Lou, X.; Yang, C.; Li, D.; Zhang, Y. PEEK (Polyether-ether-ketone) and its composite materials in orthopedic implantation. *Arab. J. Chem.* **2021**, *14*, 102977. [[CrossRef](#)]
57. Rezaei, F.; Hassani, K.; Solhjoei, N.; Karimi, A. Carbon/PEEK composite materials as an alternative for stainless steel/titanium hip prosthesis: A finite element study. *Australas. Phys. Eng. Sci. Med.* **2015**, *38*, 569–580. [[CrossRef](#)]
58. Carpenter, R.D.; Klosterhoff, B.S.; Torstrick, F.B.; Foley, K.T.; Burkus, J.K.; Lee, C.S.D.; Gall, K.; Guldborg, R.E.; Safranski, D.L. Effect of porous orthopaedic implant material and structure on load sharing with simulated bone ingrowth: A finite element analysis comparing titanium and PEEK. *J. Mech. Behav. Biomed. Mater.* **2018**, *80*, 68–76. [[CrossRef](#)]
59. Anguiano-Sanchez, J.; Martinez-Romero, O.; Siller, H.R.; Diaz-Elizondo, J.A.; Flores-Villalba, E.; Rodriguez, C.A. Influence of PEEK Coating on Hip Implant Stress-shielding: A Finite Element Analysis. *Comput. Math. Methods Med.* **2016**, *2016*, 6183679. [[CrossRef](#)]
60. Darwich, A.; Nazha, H.; Daoud, M. Effect of Coating Materials on the Fatigue Behavior of Hip Implants: A Three-dimensional Finite Element Analysis. *J. Appl. Comput. Mech.* **2020**, *6*, 284–295.
61. Nakahara, I.; Takao, M.; Bandoh, S.; Bertollo, N.; Walsh, W.R.; Sugano, N. In vivo implant fixation of carbon fiber-reinforced PEEK hip prostheses in an ovine model. *J. Orthop. Res.* **2013**, *31*, 485–492. [[CrossRef](#)]
62. Tavakkoli, A.P.; Samiezadeh, S.; Klika, V.; Bougherara, H. Investigating stress-shielding spanned by biomimetic polymer-composite vs. metallic hip stem: A computational study using mechano-biochemical model. *J. Mech. Behav. Biomed. Mater.* **2015**, *41*, 56–67. [[CrossRef](#)]
63. Zhang, L.; Song, B.; Choi, S.-K.; Shi, Y. A topology strategy to reduce stress-shielding of additively manufactured porous metallic biomaterials. *Int. J. Mech. Sci.* **2021**, *197*, 106331. [[CrossRef](#)]
64. Hsiang Loh, G.; Pei, E.; Harrison, D.; Monzón, M.D. An overview of functionally graded additive manufacturing. *Addit. Manuf.* **2018**, *23*, 34–44. [[CrossRef](#)]
65. Naebe, M.; Shirvanimoghaddam, K. Functionally graded materials: A review of fabrication and properties. *Appl. Mater. Today* **2016**, *5*, 223–245. [[CrossRef](#)]
66. Shi, H.; Zhou, P.; Li, J.; Liu, C.; Wang, L. Functional Gradient Metallic Biomaterials: Techniques, Current Scenery, and Future Prospects in the Biomedical Field. *Front. Bioeng. Biotechnol.* **2021**, *18*, 616845. [[CrossRef](#)]
67. Sola, A.; Bellucci, D.; Cannillo, V. Functionally graded materials for orthopedic applications—An update on design and manufacturing. *Biotechnol. Adv.* **2016**, *34*, 504–531. [[CrossRef](#)]
68. Gok, M.G. Creation and finite-element analysis of multi-lattice structure design in hip stem implant to reduce the stress-shielding effect. *Proc. Inst. Mech. Eng. Part L J. Mater. Des. Appl.* **2022**, *236*, 429–439. [[CrossRef](#)]

69. Trevisan, F.; Calignano, F.; Aversa, A.; Marchese, G.; Lombardi, M.; Biamino, S.; Ugues, D.; Manfredi, D. Additive manufacturing of titanium alloys in the biomedical field: Processes, properties and applications. *J. Appl. Biomater. Funct. Mater.* **2018**, *16*, 57–67. [[CrossRef](#)] [[PubMed](#)]
70. Murr, L.E.; Gaytan, S.M.; Medina, F.; Lopez, H.; Martinez, E.; Machado, B.I.; Hernandez, D.H.; Martinez, L.; Lopez, M.I.; Wicker, R.B.; et al. Next-generation biomedical implants using additive manufacturing of complex, cellular and functional mesh arrays. *Philos. Trans. A Math. Phys. Eng. Sci.* **2010**, *368*, 1999–2032. [[CrossRef](#)]
71. Oshkour, A.A.; Abu Osman, N.A.; Yau, Y.H.; Tarlochan, F.; Abas, W.A. Design of new generation femoral prostheses using functionally graded materials: A finite element analysis. *Proc. Inst. Mech. Eng. H* **2013**, *227*, 3–17. [[CrossRef](#)]
72. Ahirwar, H.; Sahu, A.; Gupta, V.K.; Kumar, P.; Nanda, H.S. Design and finite element analysis of femoral stem prosthesis using functional graded materials. *Comput. Methods Biomech. Biomed. Eng.* **2021**, *23*, 1–14. [[CrossRef](#)]
73. Al-Jassir, F.F.; Fouad, H.; Alothman, O.Y. In vitro assessment of Function Graded (FG) artificial Hip joint stem in terms of bone/cement stresses: 3D Finite Element (FE) study. *Biomed. Eng. Online* **2013**, *12*, 5. [[CrossRef](#)] [[PubMed](#)]
74. Chowdhury, S.; Anand, A.; Singh, A.; Pal, B. Evaluation of mechanical properties of Ti-25Nb BCC porous cell structure and their association with structure porosity: A combined finite element analysis and analytical approach for orthopedic application. *Proc. Inst. Mech. Eng. H* **2021**, *235*, 827–837. [[CrossRef](#)] [[PubMed](#)]
75. Hazlehurst, K.B.; Wang, C.J.; Stanford, M. The potential application of a Cobalt Chrome Molybdenum femoral stem with functionally graded orthotropic structures manufactured using Laser Melting technologies. *Med. Hypotheses* **2013**, *81*, 1096–1099. [[CrossRef](#)]
76. Abdelaal, O.; Darwish, S.; El-Hofy, H.; Saito, Y. Patient-specific design process and evaluation of a hip prosthesis femoral stem. *Int. J. Artif. Organs* **2019**, *42*, 271–290. [[CrossRef](#)] [[PubMed](#)]
77. Jiang, M.; Coles-Black, J.; Chen, G.; Alexander, M.; Chuen, J.; Hardidge, A. 3D Printed Patient-Specific Complex Hip Arthroplasty Models Streamline the Preoperative Surgical Workflow: A Pilot Study. *Front. Surg.* **2021**, *8*, 687379. [[CrossRef](#)] [[PubMed](#)]
78. Haglin, J.M.; Eltorai, A.E.; Gil, J.A.; Marcaccio, S.E.; Botero-Hincapie, J.; Daniels, A.H. Patient-Specific Orthopaedic Implants. *Orthop. Surg.* **2016**, *8*, 417–424. [[CrossRef](#)] [[PubMed](#)]
79. Jacquet, C.; Flecher, X.; Pioger, C.; Fabre-Aubrespy, M.; Ollivier, M.; Argenson, J.N. Long-term results of custom-made femoral stems. *Orthopade* **2020**, *49*, 408–416. [[CrossRef](#)]
80. Fontalis, A.; Epinette, J.A.; Thaler, M.; Zagra, L.; Khanduja, V.; Haddad, F.S. Advances and innovations in total hip arthroplasty. *SICOT J.* **2021**, *7*, 26. [[CrossRef](#)]
81. Bartlett, J.D.; Lawrence, J.E.; Stewart, M.E.; Nakano, N.; Khanduja, V. Does virtual reality simulation have a role in training trauma and orthopaedic surgeons? *Bone Jt. J.* **2018**, *100-B*, 559–565. [[CrossRef](#)]
82. Clarke, E. Virtual reality simulation—The future of orthopaedic training? A systematic review and narrative analysis. *Adv. Simul.* **2021**, *6*, 2. [[CrossRef](#)]
83. Rivière, C.; Harman, C.; Logishetty, K.; Van Der Straeten, C. Hip Replacement: Its Development and Future. In *Personalized Hip and Knee Joint Replacement [Internet]*; Rivière, C., Vendittoli, P.A., Eds.; Springer: Cham, Switzerland, 2020; Chapter 3.
84. Marsh, M.; Newman, S. Trends and developments in hip and knee arthroplasty technology. *J. Rehabil. Assist. Technol. Eng.* **2021**, *8*, 2055668320952043. [[CrossRef](#)] [[PubMed](#)]